Dental Materials xxx (xxxx) xxx

Contents lists available at ScienceDirect

Dental Materials

journal homepage: www.elsevier.com/locate/dental

Emerging technologies for the evaluation of spatio-temporal polymerisation changes in flowable vs. sculptable dental resin-based composites

Danijela Marovic [a], Håvard J. Haugen [b], Matej Par [a], Stefanie Linskens [b,c], Emile Mensikova [b], Visnja Negovetic Mandic [a], Sander Leeuwenburgh [c], Liebert P. Nogueira [d], Pekka K. Vallittu [e], Qianli Ma [b,*]

[a] Department of Endodontics and Restorative Dentistry, School of Dental Medicine, University of Zagreb, Croatia
[b] Department of Biomaterials, Institute of Clinical Dentistry, University of Oslo, Norway
[c] Department of Dentistry – Regenerative Biomaterials, Radboud University Medical Center, Nijmegen, the Netherlands
[d] Oral Research Laboratory, Institute of Clinical Dentistry, University of Oslo, Norway
[e] Department of Biomaterials Science, Institute of Dentistry, University of Turku and Welfare District of South-West Finland, Turku, Finland

ARTICLE INFO

Keywords:
Dental composite resins
Polymerisation shrinkage
Micro-CT
Optical photothermal infrared spectroscopy
O-PTIR
Filler content
Degree of conversion
Flowable

ABSTRACT

Background: This study presents a novel multi-technique approach that integrates micro-CT and optical photothermal infrared spectroscopy (O-PTIR) to evaluate polymerisation differences, so-called spatio-temporal polymerisation properties, between flowable and sculptable dental resin-based composites.
Methods: Ten commercially available dental composites were investigated, including flowable and sculptable counterparts from the same manufacturer. Eight parameters were evaluated: short-term polymerisation characteristics (degree of conversion after 5 min, maximum polymerisation rate, time to reach maximum polymerisation rate) was measured using ATR-FTIR with real-time monitoring; changes in the degree of conversion with depth were evaluated with O-PTIR, 3D visualisation of shrinkage patterns, overall volumetric shrinkage, depth-specific shrinkage, and porosity were measured using micro-CT; surface morphology with detailed measurements of elemental composition was characterised using SEM/EDX; light transmittance was analysed with a NIST-referenced spectrometer.
Results: The study found that the increase in filler weight and volume ratio reduced the degree of conversion and polymerisation shrinkage, while moderately influencing the maximum polymerisation rates. The time to reach maximum polymerisation rates and light transmittance were not dependent on the filler amount. O-PTIR assessed a depth-dependent decrease in the degree of conversion for both composite types, with flowable composites generally showing a greater decrease in the degree of conversion than sculptable composites, except for bulk-fill composites. Micro-CT scans showed significantly higher flowable shrinkage values than their sculptable counterparts, highlighting the performance differences between the two types of composites.
Conclusions: The findings of this study have practical implications for the selection and use of dental composites. Flowable composites, despite their higher degrees of conversion and polymerisation rates, also exhibit higher volumetric shrinkage, which can be detrimental for clinical applications. The new measurement methods used in this study provide a comprehensive overview of the polymerisation behaviour of commercially available dental composites, offering valuable insights for material optimisation.

1. Introduction

The continuous development of resin-based composite (RBC) materials aims to improve the effectiveness and longevity of dental restorations – a crucial aspect of contemporary dentistry. However, dentists prioritise aesthetic results and ease of use when selecting materials for their practice. These goals have led to significant modifications in RBC formulations over the years, whether in the filler or resin phase.

However, challenges such as polymerisation shrinkage (PS), insufficient degree of conversion (DC) and suboptimal mechanical properties still hinder the longevity of RBC restorations [1]. A high DC of RBCs is associated with improved mechanical properties [2,3], reduced adverse

* Corresponding author.
E-mail address: qianlima@odont.uio.no (Q. Ma).

https://doi.org/10.1016/j.dental.2024.09.002
Received 18 June 2024; Received in revised form 30 August 2024; Accepted 10 September 2024

effects due to leaching of the unpolymerised monomers [4], reduced bacterial adhesion [5], better wear resistance [6] and colour stability [7], etc. One negative consequence must be considered when attempting to achieve maximum polymerisation, i.e. shrinkage [2]. Loss of volume after polymerisation of the dimethacrylate polymer network is currently an unavoidable problem, leading to the formation of internal stresses in a bonded cavity and localised detachment of the restoration from the tooth structure defined as marginal gaps. Marginal gaps larger than 60 μm are considered predictive indicators of secondary caries [8–10]. Therefore, it is necessary to understand the dynamic mechanisms of changes in polymerisation and shrinkage over time and space to find possible solutions to these problems.

Polymerisation properties such as DC, PS and even light transmission are subject to dynamic changes that start with the illumination of the polymerised surface and continue long after 24 h post-cure [11,12]. Although most monomers are linked in the polymer network in the first few seconds after illumination, as revealed by the DC measurements, the PS lags behind and shows its maximum in twice the time needed for the DC [13]. In addition, the light emitted by the curing device is reflected at the sample surface, scattered by the filler particles in the RBC and absorbed by the photoinitiators in the RBC areas closest to the light source, reducing the chances of activating the photoinitiators at deeper parts of the sample [14,15]. The consequence is a gradual decrease in DC, crosslink density of the polymer network and PS with increasing distance from the light source [2,3]. These parameters are often quantified macroscopically at the level of the whole sample, but the actual values are locally and temporally specific. Therefore, a comprehensive investigation of the spatio-temporal changes of the polymerisation-related parameters is required to understand better the spatial and temporal variations of the polymerising network evolution.

Flowable and sculptable RBCs traditionally represent two main categories with different properties and applications. This study investigates and compares the performance of a wide range of RBC materials to gain insights into their polymerisation-related properties.

Sculptable RBCs are generally intended for more extensive restorations and offer the possibility of easily modelling the restoration due to their paste-like consistency. Manufacturers advertise a variety of options to meet all requirements and clinical indications: highly-packed filled posterior composites that can withstand high mechanical stresses, anterior composites with specific optical properties that either block or transmit light and ensure high polishability, bulk-fill RBCs designed for rapid application in 4 mm thick layers with increased light transmittance and depth of cure, or simply “universal” RBCs with balanced properties suitable for most purposes. Due to their high filler content, sculptable RBCs are generally characterised by a high viscosity. These composites usually have a lower PS [16] but may have problems achieving a uniform DC at greater depths due to the strong light attenuation caused by the filler particles [17].

Flowable composites, on the other hand, are known for their lower viscosity, ease of application and better adaptability to cavity walls. Their lower viscosity results either from using a lower amount of filler or from using more viscous monomers in the composition. Despite their advantages, flowable composites often have a higher PS value, which can compromise the marginal integrity of the restoration [16]. Until recently, flowable RBCs were only considered suitable for small restorations and as liners under sculptable composites. However, modern formulations of flowable RBCs contain higher amounts of filler, and the manufacturers have even extended the indication to Class I and II restorations [18,19].

These new modifications blur the differences between sculptable and flowable RBCs and emphasise the diversity of composite formulations. Since material scientists do not know the exact composition of the RBCs due to the manufacturers’ trade secrets, they cannot draw clear conclusions about the relationships between composition and properties. Therefore, it is necessary to test the new materials on the dental market independently of the manufacturers’ laboratories.

Our recent study evaluated the applicability of the new investigation methods for DC and PS on a series of experimental microhybrid composites with systematically increasing filler content in 5 wt% increments [20]. A clear negative correlation was found between the filler content on one side and the DC, PS, maximum polymerisation rate and maximum shrinkage rate. The study used advanced analytical techniques such as micro-computed tomography (micro-CT) and optical photothermal infrared spectroscopy (O-PTIR) to evaluate the experimental RBCs comprehensively. Micro-CT provides detailed three-dimensional visualisations of volumetric PS and porosity, while O-PTIR enables precise measurements of DC through different depths of cure. At the same time, ATR-FTIR provides real-time measurements of polymerisation characteristics. These techniques enable an in-depth analysis of the polymerisation-related properties of dental composites and provide information for the optimisation of materials for clinical use. Thus, the same approach and analytical techniques are used in the present study with commercial flowable and sculptable RBCs.

O-PTIR is a new spectroscopic technique that is claimed to enable simultaneous IR and Raman spectroscopic measurements in non-contact (and therefore non-destructive) mode with a quality comparable to IR spectra of thin samples in transmission mode [21]. O-PTIR simultaneously uses a pulsed IR source (usually a quantum cascade laser) to excite the sample and a visible wavelength probe laser to detect the response of the sample. Both lasers are focussed on the same point through a microscope objective, and the detectors record the changes in reflectance and/or transmittance as a result of thermal expansion and change in refractive index [22]. Shortly after its market launch, it has found its application in the fields of life sciences, microplastics, forensics and polymer science [21]. However, as far as the authors are aware, there is currently no paper describing its use in dentistry.

O-PTIR offers several advantages in the assessment of dental composites. First, the high spatial resolution, often down to 100–500 nm, allows detailed mapping of DC in heterogeneous composite structures [5,23]. This precision helps identify the spatial DC variations in the polymer network. Second, the non-destructive nature of O-PTIR ensures that samples remain intact for further analysis or testing. This technique also minimises scattering effects and provides more precise and more accurate measurements compared to conventional methods such as FTIR [23].

The main objective of this study is to appraise the effectiveness of O-PTIR and micro-CT to describe the performance differences between flowable and sculptable commercial RBCs of the same brand and similar resin composition using an identical multi-technique approach as in our previous study on experimental RBCs. The parameters investigated include light transmittance, real-time polymerisation characteristics, DC changes over depth, overall PS, PS changes over depth, porosity, elemental composition and surface morphology. By integrating these eight techniques, this study aims to comprehensively understand commercial RBCs’ behaviour and investigate their interrelationships. The study hypothesises that flowable composites have higher DC, faster polymerisation rates, and higher PS than sculptable composites.

2. Materials and methods

2.1. Materials

This study used ten commercially available dental resin composites with different resin/filler ratios, as shown in Table 1.

3. Characterisation with SEM-EDX

The surface morphology of polymerised dental RBCs was visualised using scanning electron microscopy (SEM). This investigation was complemented by energy-dispersive X-ray spectroscopy (EDX) to quantify the samples’ elemental composition. The SEM analyses were performed at an accelerating voltage of 15 kV and a magnification of

Table 1
Composition of the dental composites used in the study, as provided by the manufacturers.

Flowable				Sculptable			
Product (shade)	Indication	Resin	Filler content	Product (shade)	Indication	Resin	Filler content
Charisma Flow (A2)	Conv. Class V, Small Class I–III	E2BADMA TEGDMA	61.5 wt% 38 vol%	**Charisma Classic (A2)**	Conv. Universal Class I–V	Bis-GMA, TEGDMA, UDMA	77.5 wt% 61 vol%
G-ænial Universal Flow (A2)	Conv. Class I–V	UDMA, Bis-MEPP, TEGDMA	69 wt% 50 vol%	**G-ænial Posterior (P-A2)**	Conv. Class I and II	UDMA, DMA monomers	77 wt% 65 vol%
Brilliant EverGlow Flow (A2/B2)	Conv. Small Class III and V, liner	Bis-GMA, Bis-EMA	65 wt% 46 vol%	**Brilliant EverGlow (A2/B2)**	Conv. Class I–V	Bis-GMA, TEGDMA	79 wt% 64 vol%
Filtek Restorative SupremeFlowable (A2)	Conv. Class I–V	Bis-GMA, TEGDMA, Bis-EMA	65 wt% 46 vol%	**Filtek Restorative Supreme XTE Universal (A2B)**	Conv. Class I–V Indirect restorations	bis-GMA, UDMA, TEGDMA, bis-EMA, PEGDMA	78.5 wt% 63.3 vol%
Filtek Restorative Bulk Fill Flowable (A2)	Bulk-fill Base under Class I, II, Small Class III and V	Bis-GMA, UDMA, Bis-EMA	64.5 wt% 42.5 vol%	**Filtek Restorative One Bulk Fill (A2)**	Bulk-fill Class I–V Indirect restorations	AFM, AUDMA, UDMA, 1, 12-dodecane-DMA	76.5 wt% 58.5 vol%

* E2BADMA: bisphenol A ethoxylate dimethacrylate alkoxylated with 2 ethylene oxide units; Bis-GMA: bisphenol-A-glycidylmethacrylate, Bis-EMA: ethoxylated bisphenol A dimethacrylate; UDMA: urethane dimethacrylate; TEGDMA: triethylene glycol dimethacrylate; Bis-MEPP: bisphenol A ethoxylate dimethacrylate; PEGDMA: polyethylene glycol dimethacrylate; AFM: addition-fragmentation monomer; AUDMA: aromatic urethane dimethacrylate; DMA: dimethacrylate; Conven.: conventional, placed in 2-mm layers.

5000x using a Hitachi Tabletop Microscope TM3030 (Tokyo, Japan). In parallel, EDX analysis with a Quantax 70 system provided detailed element mapping, enabling a comprehensive assessment of the samples' chemical properties.

3.1. Characterisation of the curing unit and light transmittance

The identical curing unit Bluephase PowerCure (Ivoclar Vivadent, Schaan, Liechtenstein) was used for all tests in this study. The light-curing unit was characterised using the MARC System spectrometer (Bluelight Analytics Inc., Halifax, NS, Canada), referenced and calibrated with the National Institute of Standards and Technology (NIST) light source. The radiant exitance of the light curing device was measured on an empty compartment in triplicate. The radiant exposure in a wavelength range of 360–540 nm was recorded individually at a rate of 16 recordings/s. The sensor was triggered at 20 mW.

Light transmittance measurements through the tested composites were performed under the same conditions as the characterisation of the curing device. The uncured composite samples in Delrin moulds (h = 2 mm, d = 6 mm) were placed on the sensor aperture of the MARC spectrometer. The curing device was positioned centrally and perpendicular to the sample surface in a fixed position, and the samples were illuminated for 20 s. The irradiance and radiation exposure were recorded in real-time with 16 recordings/s at the bottom of the sample.

3.2. Real-time polymerisation characteristics

Polymerisation characteristics were analysed using a Fourier transform infrared (FTIR) spectrometer (Nicolet iS50, Thermo Fisher, Madison, USA) equipped with an attenuated total reflectance (ATR) accessory. Uncured composite samples (n = 5) were placed in a custom-made silicone mould (d = 6, h = 1.5 mm) covering the ATR diamond, covered with a PET foil, and subjected to a 20-second light-curing session. Real-time FTIR spectra were captured at two spectra/second over 5 min, each with four scans at an 8 cm^{-1} resolution. The DC after 5 min ($DC_{5\ min}$) was derived from the absorbance intensity ratios of aliphatic (1638 cm^{-1}) to aromatic bands (1608 cm^{-1}):

$$DC(\%)\left[1-\frac{(1638\ \ cm^{-1}/1608\ \ cm^{-1})_{peak\ height\ after\ curing}}{(1638\ \ cm^{-1}/1608\ \ cm^{-1})_{peak\ height\ before\ curing}}\right]x\ \ 100$$

The DC was charted over time to analyse reaction rates, the maximum polymerisation rate (R_{max}), and the time to reach R_{max} (t_{Rmax}).

3.3. Degree of conversion at different depths

Optical photothermal infrared spectroscopy (O-PTIR) with a mIRage system (Photothermal Spectroscopy Corp., Santa Barbara, California, USA) was used to measure the DC values in the tested composites with increasing thickness of the composite. This device utilises four quantum cascade laser chips that emit specific infrared wavelengths in the range of 770–1802 cm^{-1}. The resulting photothermal expansions in the samples were detected using a green laser with a wavelength of 532 nm and an avalanche photodiode. A Cassegrain objective with a numerical aperture of 0.78 was used, resulting in a size of the green laser spot (and thus a spatial resolution) of 416 nm on the sample. The IR and Raman spectra were recorded as 3 averaged scans per measurement spot. Three measurement spots were selected for each sample (n = 5): 0 mm (below the surface), 2 mm and 4 mm.

The spectra with absorbance peaks at 1638 cm^{-1} and 1609.4 cm^{-1} corresponding to aliphatic and aromatic bonds, respectively, were obtained from uncured and cured samples and used to calculate the DC by comparing the ratios of aliphatic and aromatic bonds using the same formula as for ATR-FTIR.

3.4. Micro-CT scans for volumetric shrinkage assessment

As previously described, volumetric PS measurements were executed by encasing the dental composites in orange-filtered tubes for micro-CT scanning [24]. Cylindrical samples (d = 2 mm h = 2 mm) were scanned pre- and post-curing using a SkyScan 1172 (Bruker, Kontich, Belgium) under specific conditions for precise image superimposition (n = 3). Scans were reconstructed and analysed using NRecon software for initial adjustments and Avizo for 3D reconstructions, with subsequent analysis via CTAn software to evaluate volumetric shrinkage and porosity, ensuring enhanced image clarity and artefact reduction.

3.5. Statistical analysis

Data distribution was first assessed for normality using the Kolmogorov–Smirnov test, followed by a Holm-Sidak method for normality verification, presenting data as means with standard deviation if normal distributed and median with interquartile range if not. Both one-way

and two-way ANOVA and Tukey's post-hoc tests were utilised for parametric dataset comparison. Mann-Whitney test was used for the non-parametric dataset. Spearman Rank Correlation analysis was used to investigate the relationships between the investigated parameters. Datasets were considered significantly different for $p < 0.05$. All statistical analyses were conducted using GraphPad Prism version 10, with significance levels predetermined.

4. Results

4.1. SEM-EDX

The samples displayed a uniform distribution of elements on their filler surfaces. It is worth noting that the flowable and sculptable materials of the same brand had similar filler shapes and sizes, except Charisma Classic, which has larger 2–5 μm particles than the corresponding flowable material. The Brilliant EverGlow and Brilliant EverGlow Flow materials, as well as Filtek One Restorative Bulk fill and Filtek Restorative Bulk Fill Flow, show the presence of submicron particles. The distribution of silicon and barium showed that the glass particles present were homogeneously distributed in all samples.

4.2. Characterisation of the curing unit and light transmittance

The light guide of the Bluephase PowerCure curing unit had a 9 mm diameter and an emission in the range of 360–540 nm with wavelength maxima at 411 and 450 nm. The measured radiant exitance at the high-power mode amounted to 734 mW/cm^2.

There was neither a group-specific behaviour in the **light transmittance** of sculptable and flowable materials nor a consistent, statistically significant difference between materials of the same brand (Figs. 1 and 2). Sculptable Brilliant EverGlow had the lowest light transmittance (1.39 ± 0.34 %) and Filtek Restorative Bulk Fill Flowable (5.52 ± 0.59 %) among all materials tested. In the group of sculptable

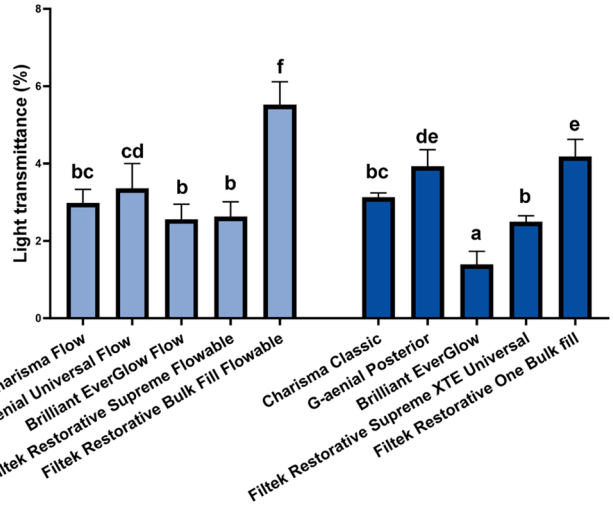

Fig. 2. Light transmission (mean ± s.d.) of the flowable and sculptable composites, identical letters denote statistically homogeneous groups Statistical significance exists between different letters ($p < 0.05$).

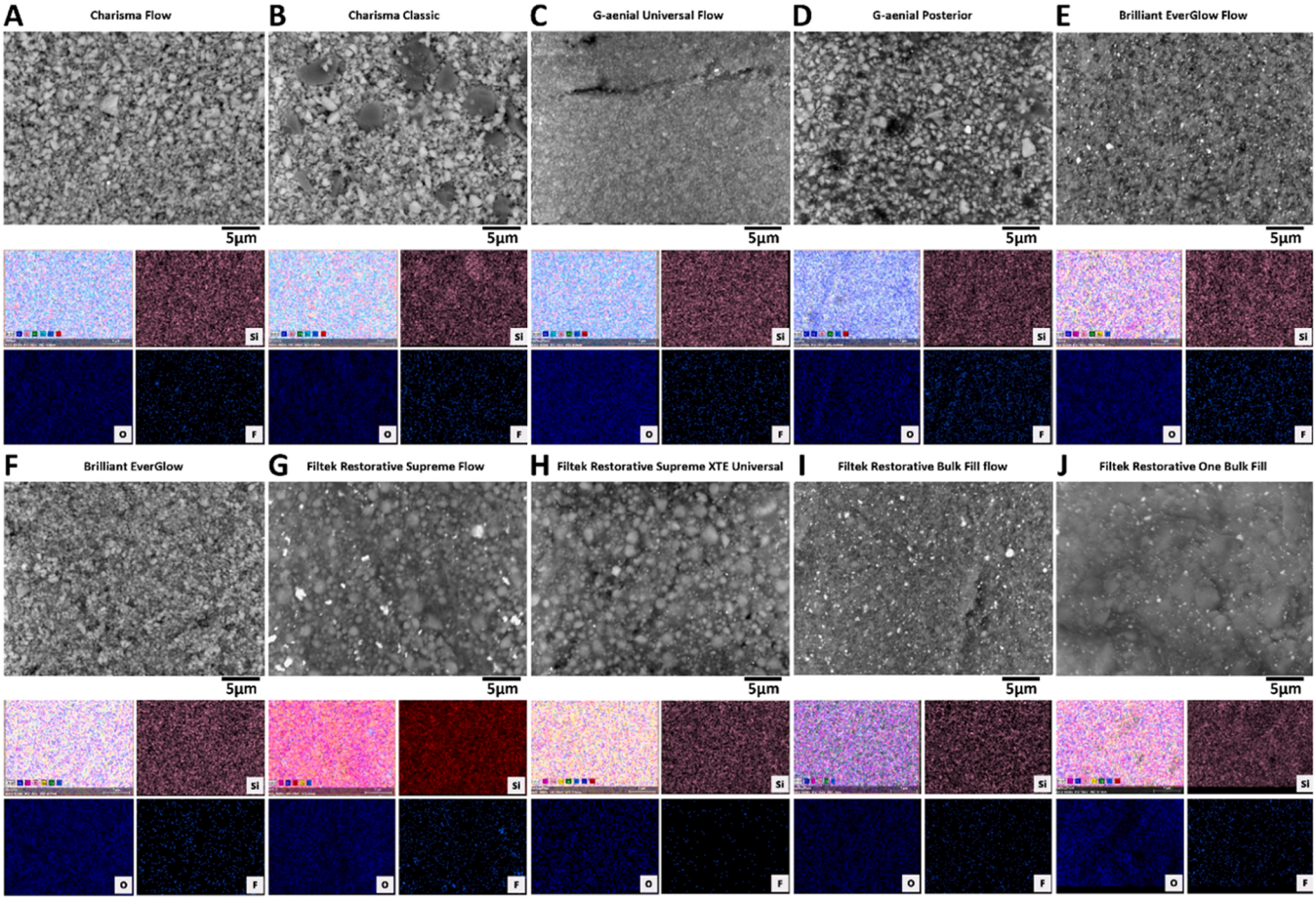

Fig. 1. Surface morphology and elemental mapping images of commercial dental composites. Silica (Si), Oxygen (O), and fluorine (F) were mapped via EDX assay. Scale bar = 5 μm.

materials, G-aenial Posterior (3.93 ± 0.43 %) and Filtek One Bulk Fill (4.18 ± 0.44 %) showed the highest light transmittance with no significant difference. Among the flowable composites, Brilliant EverGlow Flow and Filtek Supreme Flow showed the lowest light transmittance (2.56 ± 0.39 % and 2.63 ± 0.39 % respectively).

4.3. Real-time polymerisation characteristics

The polymerisation characteristics 5 min post-light curing at the bottom of the 1.5 mm high specimens are shown in Fig. 3.

Fig. 4 shows the quantitative polymerisation characteristics: $DC_{5\ min}$, R_{max} and t_{Rmax}. Overall, the **$DC_{5\ min}$** showed higher values for flowable vs. sculptable materials of the same brand. The $DC_{5\ min}$ for flowable materials ranged from 58.78 ± 2.06 % for Charisma Flow to 67.10 ± 1.27 % for Brilliant EverGlow Flow. G-aenial Posterior had the lowest $DC_{5\ min}$ (37.86 ± 0.93 %) of all materials tested, while Filtek One Bulk Fill had the highest $DC_{5\ min}$ of the sculptable composites (47.06 ± 1.54 %). Notably, the highest **R_{max}**, maximum polymerisation rate, was recorded for Filtek One Bulk Fill Flowable (11.1 ± 0.84 %/s) and G-aenial Universal Flow (10.61 ± 1.80 %/s). The R_{max} was also generally quicker for the flowable materials, except for Charisma Flow (3.57 ± 0.45 %/s), which was similar to sculptable materials (from 2.93 ± 0.28 %/s for Brilliant EverGlow to 4.63 ± 0.88 %/s for Charisma Classic).

Accordingly, **t_{Rmax}**, the time period required for each material to reach its maximum polymerisation rate, was the longest for Brilliant EverGlow (4.61 ± 0.82 s) and Brilliant EverGlow Flow (5.08 ± 1.77 s) and shortest for Filtek One Bulk Fill Flowable (2.12 ± 0.55 s).

4.4. DC changes over depth with O-PTIR

Fig. 5 presents detailed measurements with the O-PTIR spectroscopy at different depths. Each composite was analysed at the subsurface level – 0 mm ($DC_{0\ mm}$) and depths of 2 ($DC_{2\ mm}$) and 4 mm ($DC_{4\ mm}$). The spectra from the OPTIR (Fig S2) where similar to the FTIR measurements (Fig S4), where both showed little noise.

All materials showed a depth-dependent decline in DC measured by O-PTIR from 0 to 4 mm. Only the two bulk-fills, Filtek One Bulk Fill and Filtek Bulk Fill Flow, demonstrated no significant difference between $DC_{0\ mm}$, $DC_{2\ mm}$, and $DC_{4\ mm}$, but they showcased higher variability at 2 mm and 4 mm depths. The OPTIR spectra showed a decrease in peak intensity deeper into the samples as displayed in Fig S3.

For Brilliant EverGlow, O-PTIR measurements decrease progressively with depth, down to 34.7 ± 4.7 % (Fig. 4**C**). Brilliant EverGlow Flow and Filtek Supreme Flow also significantly reduced O-PTIR DC at 4 mm depth (39.7 ± 3.1 %). Finally, Filtek Supreme XTE Universal consistently decrees at $DC_{2\ mm}$ and $DC_{4\ mm}$ (Fig. 5**D**).

Generally, comparing the DC measured by FTIR at 1.5 mm and O-PTIR at 2 mm, FTIR reached higher values, and the standard deviation was higher with OPTIR.

4.5. Volumetric polymerisation shrinkage

Fig. 6 presents the overlay of the 3D micro-CT images of the composite sample before and after curing. Notably, all samples predominantly exhibit shrinkage at their upper sections (directed towards the curing unit), irrespective of material category.

A three-dimensional reconstruction was derived from micro-CT scans. As depicted in Fig. 6, notable PS at the bottom is observed in

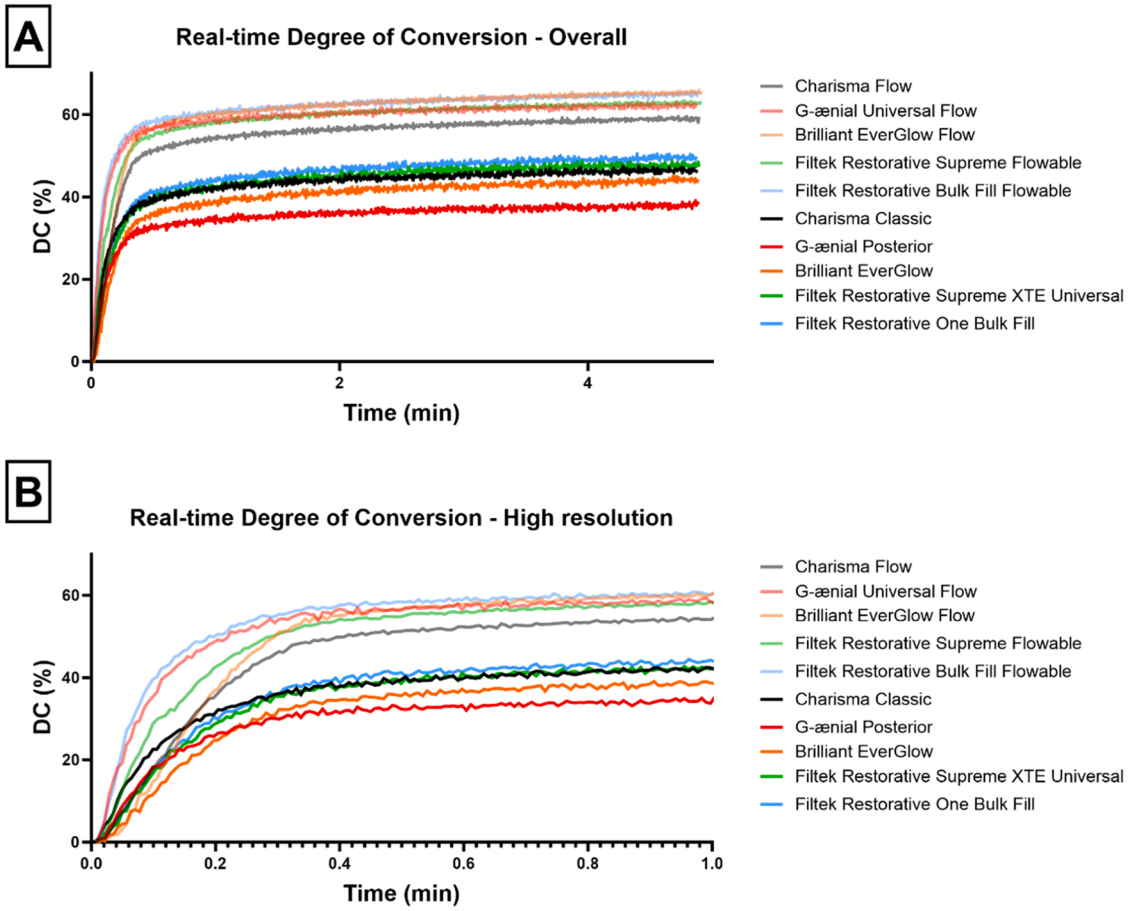

Fig. 3. Real-time development of a degree of conversion as a function of time measured by ATR-FTIR. A) overall values; B) high-resolution image.

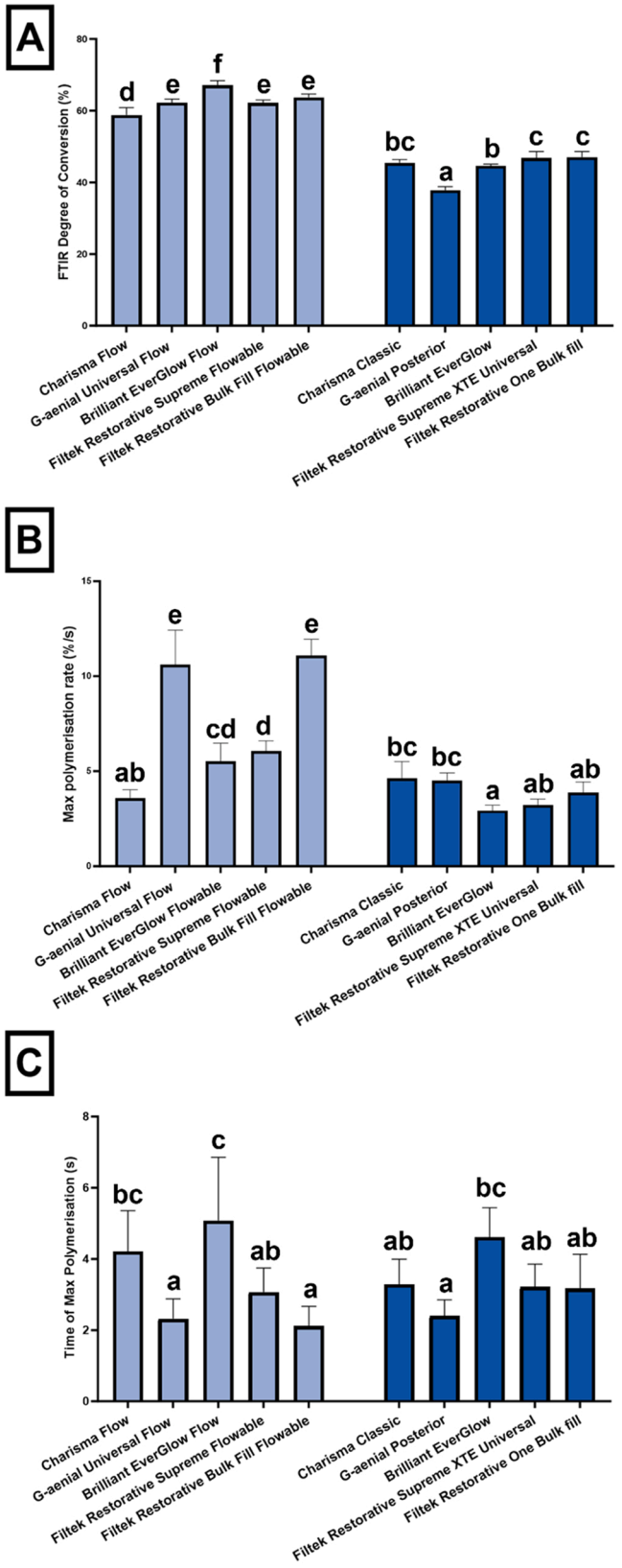

Fig. 4. Degree of conversion (A – $DC_{5\ min}$), maximum polymerisation rate (B – R_{max}) and time to reach maximum polymerisation rate (C – t_{Rmax}) (mean ± s.d.) measured by ATR-FTIR for the different composite materials at 1.5 mm depth during the first 5 min post-light curing. Statistical significance exists between different letters ($p < 0.05$).

the flowable commercial dental composites (A, C, E, G, I), with Brilliant EverGlow Flow (A) and Charisma Flow (C) displaying particularly pronounced PS at the top compared to the base of the samples. Conversely, the sculptable composites (B, D, F, H, J) exhibit reduced PS relative to the flowable varieties. Micro-CT volumetric PS measurement can produce a 3D spatial shrinkage pattern in the composite material. As the depth of curing increases, there is a noticeable reduction in PS.

Fig. 7A demonstrates the overall volumetric PS of the tested dental composites. Generally, there was a significantly higher overall PS for flowable vs. sculptable materials of the same brand. The composites with a flowable consistency, such as Gaenial Universal Flow (3.44 ± 0.17 %), Brilliant EverGlow Flow (3.81 ± 0.35 %), Filtek Bulk Fill Flowable (3.09 ± 0.26 %), Filtek Supreme Flowable (3.25 ± 0.09 %) and Charisma Flow (2.92 ± 0.31 %) show significantly higher PS compared to their sculptable counterparts, including Gaenial Posterior (1.51 ± 0.08 %), Brilliant EverGlow (1.92 ± 0.31 %), Filtek One Bulk Fill (1.46 ± 0.49 %), Filtek Supreme XTE Universal (1.53 ± 0.09 %), and Charisma Classic (1.97 ± 0.25 %). A general trend of flowable composites with higher shrinkage levels can be observed, ranging between 2.23 % and 3.81 %. On the other hand, shrinkage of sculptable materials ranged between 1.46 % and 1.97 %.

The linear regression of PS at various depths of the composites only revealed a significant regression for three groups, all of which had declining slopes vs. depth: Charisma Classic (slope = − 0.2248), Charisma Flow (slope = − 0.4316), and Filtek XTE supreme (slope = − 0.3961) (Fig. S1).

Fig. 7**B–F** presents the PS across varying depths (0.2 mm to 1.7 mm) for a range of dental composites. For Charisma Classic, PS decreases with depth, peaking at 0.7 mm and then decreasing. Charisma Flow exhibits a significant decrease in PS as depth increases, with significantly higher mean values than Charisma Classic; however (Fig. 7**B**). Brilliant EverGlow and Brilliant EverGlow Flow illustrate a similar PS trend, (Fig. 7**D**). G-aenial composites exhibit a different profile. G-aenial Universal Flow demonstrates an initial high shrinkage at the superficial depth (0.2 mm) followed by a reduction. However, due to the large standard deviation, no significant G-aenial Posterior shows much lower shrinkage across all depths than G-aenial Universal Flow (Fig. 7**C**). Filtek Supreme Flowable reveals a higher shrinkage with depth, suggesting increased polymerisation shrinkage in the deeper layers. On the other hand, Filtek Restorative XTE Universal maintains a more consistent shrinkage profile with less variance across the different depths, denoting a more uniform shrinkage behaviour (Fig. 7**E**). Filtek Bulk Fill Flowable and One Bulk Fill display no significant difference (Fig. 7**F**).

4.6. Porosity

The 3D images from Fig. 6 revealed some entrapped air bubbles; these porosities were quantified and divided into open and closed porosity groups. The highest porosity was found for G-aenial Posterior (0.800 ± 0.047 %) and Charisma Classic (0.498 % ± 0.187) (Fig. 8, **A–C)**. The other tested composite had all porosity below a mean value of 0.4 %. The lowest was Brilliant EverGlow (0.084 % ± 0.047).

4.7. Correlation analysis

This study systematically compared the performance characteristics of flowable and sculptable commercial dental composites across various parameters. Median values were emphasised to represent the central tendency, while the interquartile range (IQR), encompassing the 25–75th percentiles, provided an estimate of the dispersion or variability of the data (Fig. 9). FTIR analysis for DC showed flowable composites with a median of 62 %, with an IQR of (58.6–64.1 %). In contrast, sculptable composites showed a median of 45.6 % and an IQR of (44.3–48 %), substantially lower DC rates than flowable (Fig. 9A). DC at different depths (0 mm, 2 mm, and 4 mm) was evaluated using O-PTIR (Fig. 9B–D). At the subsurface (0 mm), the flowable composites

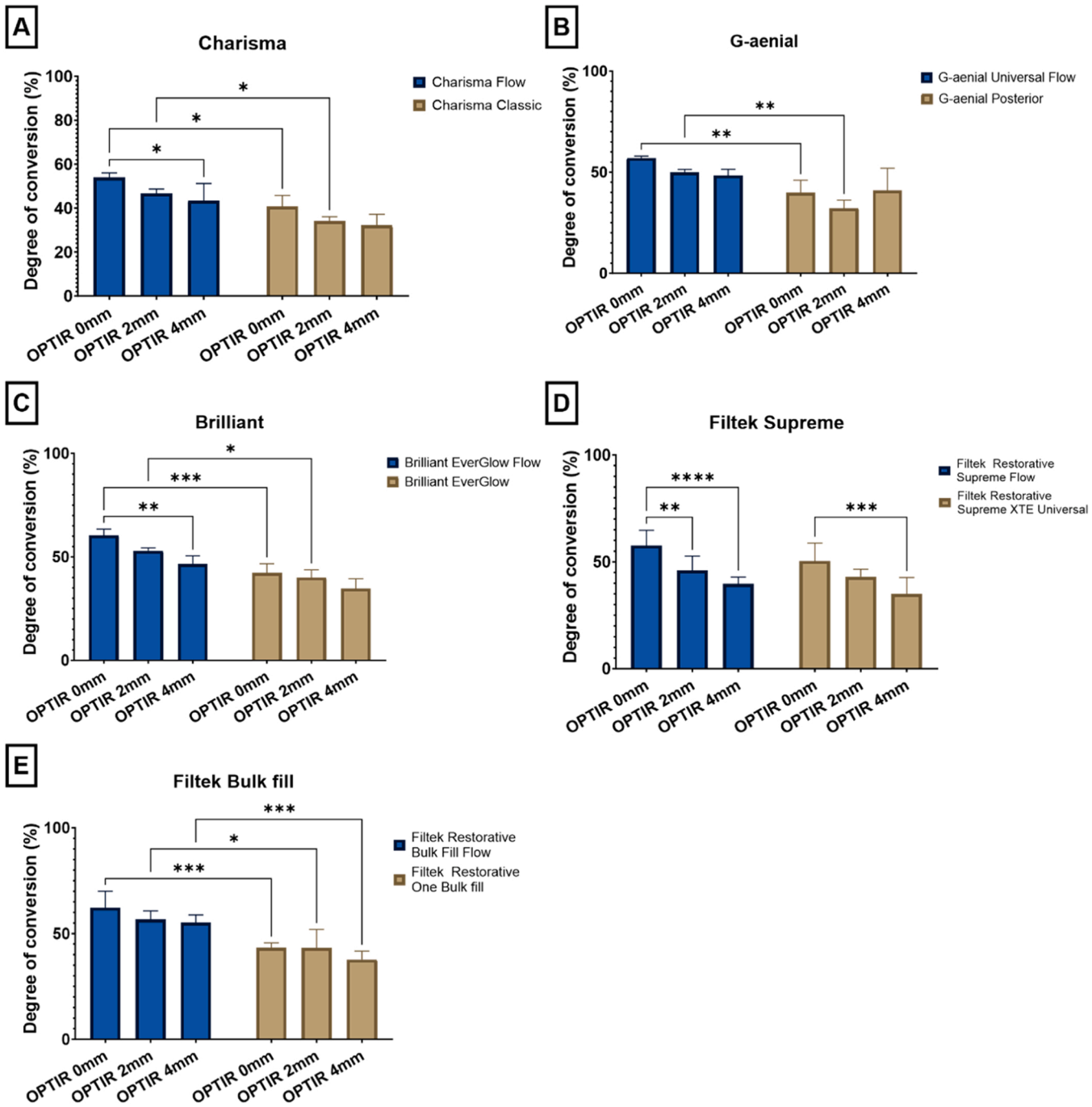

Fig. 5. Degree of conversion measured by O-PTIR at depths 0 mm ($DC_{0\ mm}$), 2 mm ($DC_{2\ mm}$) and 4 mm ($DC_{4\ mm}$) depicted as mean values ± s.d. *$p < 0.05$, **$p < 0.01$, ***$p < 0.001$, ****$p < 0.0001$.

had a median DC of 57.5 %, with an IQR of (54.7–62.7 %), while sculptable composites demonstrated a significantly lower median DC of 43.8 % and a narrower IQR of (40.4–45.9 %) (Fig. 9B). The trend of significantly higher DC in flowable composites continued at 2 mm and 4 mm depths, with medians of 48.9 % and 46.5 %, respectively, compared to sculptable composites' medians of 35.1 % and 35.6 % at the same depths. The IQR also highlighted a greater value spread for flowable composites at all depths (Fig. 9B–D).

Volumetric median PS values were 3.14 % for flowable composite vs. a significantly lower value of 1.61 % for sculptable composites, with respective IQRs of (1.87–3.25 %) and (1.54–1.89 %) (Fig. 9E). The t_{Rmax}, measured in seconds, had medians of 2.6 s for flowable and 3.2 s for sculptable composites, but no significant difference (Fig. 9F). The R_{max} was significantly higher in flowable composites, with a median of 5.35 %/s, indicating a more rapid polymerisation than sculptable composites, with a median rate of 3.7 %/s (Fig. 9G). Light transmittance exhibited a median of 3.06 % for flowable composites and 3.1 % for bulk, without significant differences.

The Spearman Rank correlation analysis, accompanied by significance levels, revealed several significant ($p < 0.05$) notable relationships between the investigated parameters in dental composites (Fig. 10). Filler Weight Percentage exhibited strong positive correlations with Filler Volume Percentage (r = 0.928), Total Porosity (r = 0.697), Open Porosity (r = 0.393, $p < 0.01$), and Closed Porosity (r = 0.657). Conversely, it showed strong negative correlations with DC FTIR (r = − 0.806), DC OPTIR at 0 mm (r = − 0.664), 2 mm (r = − 0.660), and

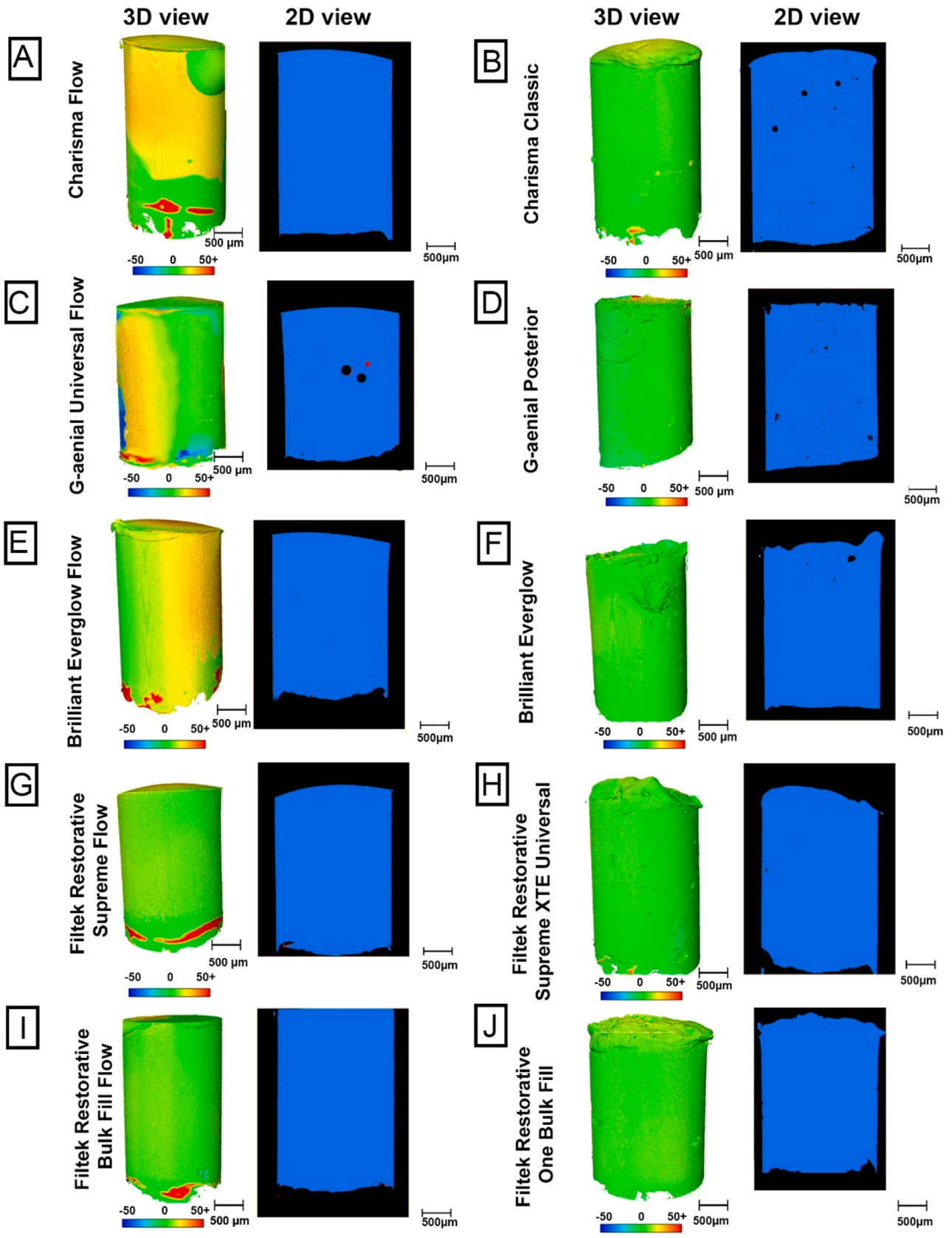

Fig. 6. Superimposed microCT of the dental composites before and after curing. The dimensional changes of flowable (A, C, E, G, I) and bulk (B, D, J, H, J) dental composites are labelled with colour spectrum (− 50 % to 50 % volumetric change). The distribution of dental composites before (red) and after polymerisation (blue) is shown in longitudinal sections (right panels in each subgraph).

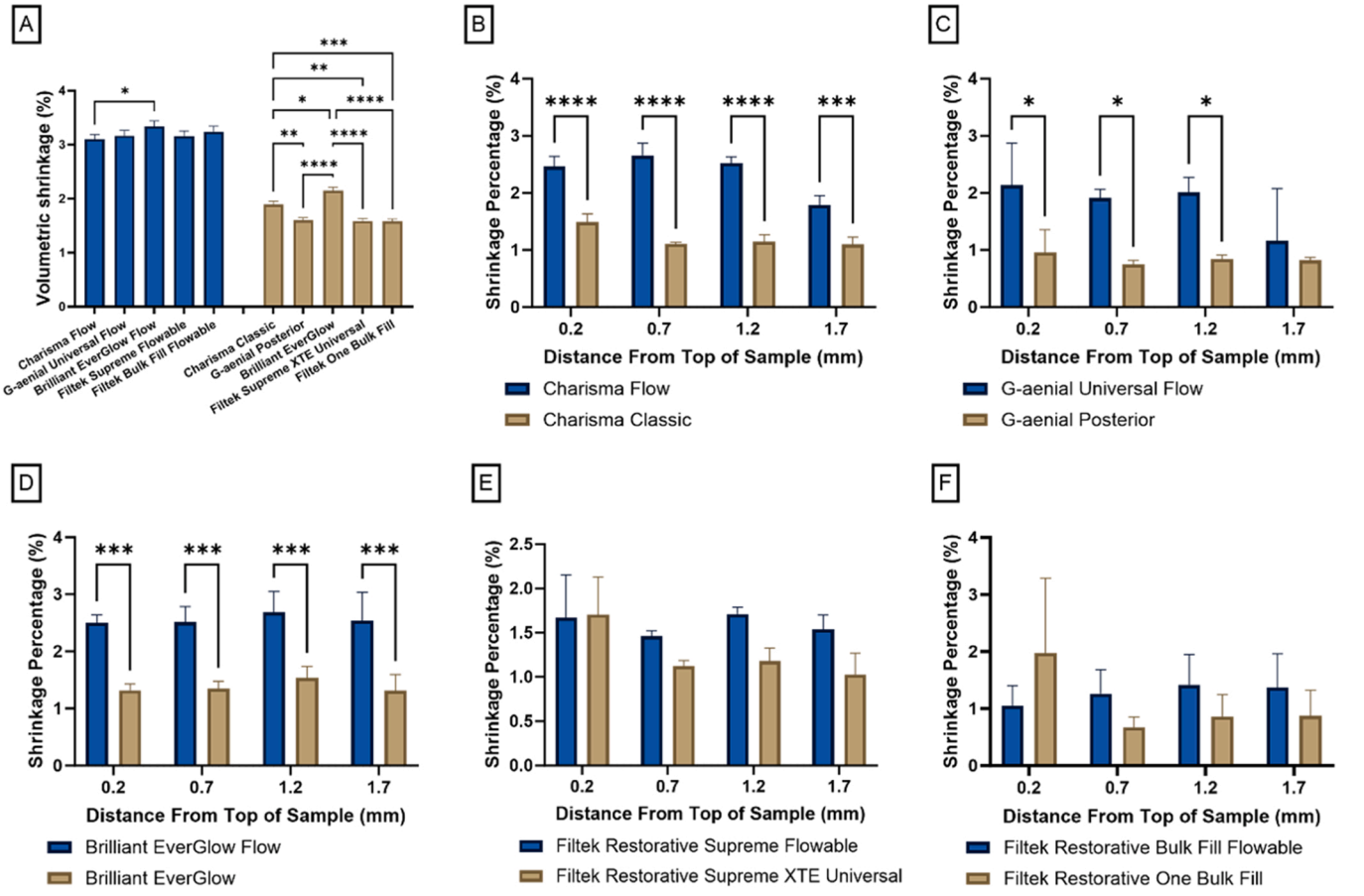

Fig. 7. Volumetric polymerisation shrinkage of commercial dental composites expressed as mean values with corresponding standard deviations (SD). (A) Overall volumetric shrinkage of flowable and sculptable composites. Significant differences existed between same-brand flowable and sculptable composites ($p < 0.0001$, not shown in the diagram for better visibility). (B-F) *$p < 0.05$, ** $p < 0.01$, *** $p < 0.001$, **** $p < 0.0001$).

4 mm (r = − 0.543), Volumetric Shrinkage (r = − 0.705), and Max Polymerisation Rate (r = − 0.443). Filler Volume Percentage demonstrated strong negative correlations with DC FTIR (r = − 0.725), DC OPTIR at 0 mm (r = − 0.617), 2 mm (r = − 0.580), and 4 mm (r = − 0.627), Volumetric Shrinkage (r = − 0.657), Total Porosity (r = 0.613) and Max Polymerisation Rate (r = − 0.531). A medium negative correlation was observed with Light Transmittance (r = − 0.355). DC FTIR had strong positive correlations with DC OPTIR at 0 mm (r = 0.822), 2 mm (r = 0.829), and 4 mm (r = 0.605), Volumetric Shrinkage (r = 0.810), and Max Polymerisation Rate (r = 0.609). It also showed strong negative correlations with Total Porosity (r = − 0.614) and Closed Porosity (r = − 0.639). DC OPTIR at 0 mm displayed strong positive correlations with DC OPTIR at 2 mm (r = 0.705) and 4 mm (r = 0.558), Volumetric Shrinkage r = 0.723), and Max Polymerisation Rate (r = 0.477). Strong negative correlations were observed with Total Porosity (r = − 0.567) and medium negative correlations with Closed Porosity (r = − 0.593). DC OPTIR at 2 mm exhibited strong positive correlations with Volumetric Shrinkage (r = 0.644) and Max Polymerisation Rate (r = 0.507). Strong negative correlations were present with Total Porosity (r = − 0.670) and Closed Porosity (r = − 0.644). DC OPTIR at 4 mm showed strong positive correlations with Volumetric Shrinkage (r = 0.672) and Max Polymerisation Rate (r = 0.546). Volumetric Shrinkage had strong positive correlations with the Max Polymerisation Rate (r = 0.546). Time of Max Polymerisation Rate demonstrated a strong negative correlation with medium negative correlations with Light Transmittance (r = − 0.457) and Open Porosity (r = − 0.300). Max Polymerisation Rate had a medium positive correlation with Light Transmittance (r = 0.449). All correlations reported above exhibited p-values < 0.01.

The Spearman Rank correlation analysis for sculptural composite (Fig. S2 A) and the significance levels highlight the most significant relationships ($p < 0.05$) between the investigated parameters. Filler Weight Percentage positively correlated with Total Porosity (r = 0.460, $p = 0.010$). A medium positive correlation was found with the Filler Volume Percentage (r = 0.400). Filler Volume Percentage showed a strong positive correlation with Volumetric Shrinkage (r = 0.622) and a medium positive correlation with Time of Max Polymerisation Rate (r = 0.515). Additionally, it demonstrated a strong negative correlation with Light Transmittance (r = − 0.948). DC FTIR had a strong positive correlation with DC OPTIR at 2 mm (r = 0.618). It also showed strong negative correlations with Total Porosity (r = − 0.489) and Closed Porosity (r = − 0.532). DC OPTIR at 2 mm exhibited a strong positive correlation with DC FTIR (r = 0.618). Volumetric Shrinkage had a medium positive correlation with and a strong negative correlation with Light Transmittance (r = − 0.550). Max Polymerisation Rate demonstrated a strong negative correlation with Time of Max Polymerisation Rate (r = − 0.684) and a strong positive correlation with Light Transmittance (r = 0.606). Total Porosity positively correlated with Filler Weight Percentage (r = 0.460).

The Spearman Rank correlation analysis for flowable composite (Fig. S2 B) and the significance levels highlight the most significant relationships between the investigated parameters. Here, the significant correlations ($p < 0.05$) are reported: Filler Weight Percentage positively correlated with Total Porosity (r = 0.559). Additionally, it showed medium positive correlations with Filler Volume Percentage (r = 0.400), Max Polymerisation Rate (r = 0.458), and Open Porosity (r = 0.422). Filler Volume Percentage showed strong positive correlations with Volumetric Shrinkage (r = 0.554), Time of Max

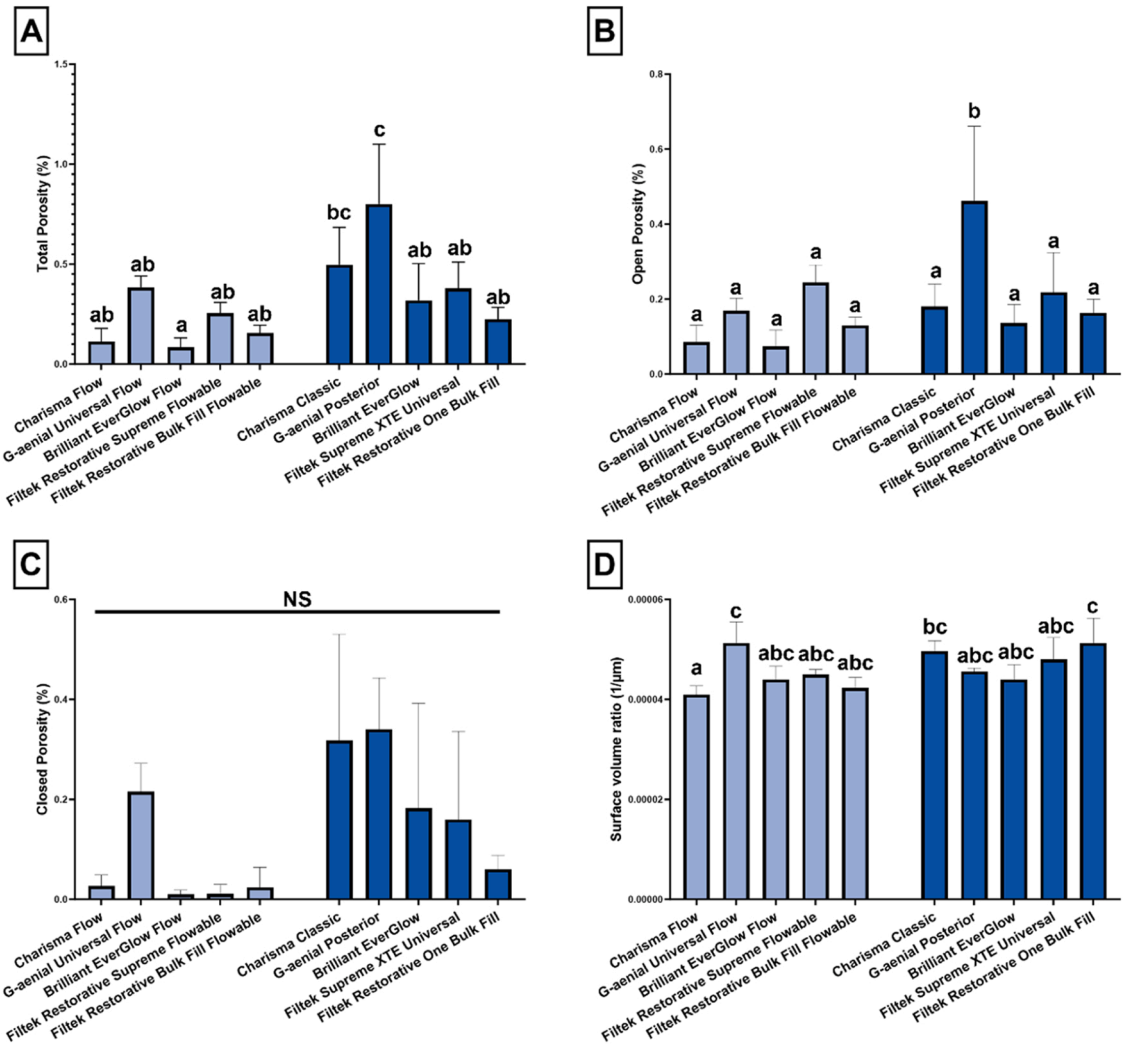

Fig. 8. Porosity measurement of tested dental composites: (A) total porosity, (B) percentage of open porosity, (C) a percentage of closed porosity, (D) Surface and volume ratio. (A- D) were calculated by using micro-CT and Avizo 3D Software ver. 2022.1. Data are presented as an average of three samples with a standard deviation; Statistical significance exists between different letters ($p < 0.05$). Identical letters denote statistically homogeneous groups ($p > 0.05$).NS, no significance.

Polymerisation Rate (r = 0.450), and Closed Porosity (r = 0.562). Additionally, it demonstrated a strong negative correlation with Light Transmittance (r = − 0.906). DC FTIR had strong positive correlations with Volumetric Shrinkage (r = 0.686) and DC OPTIR at 2 mm (r = 0.618). It also showed strong negative correlations with Total Porosity (r = − 0.489) and Closed Porosity (r = − 0.532). DC OPTIR at 2 mm exhibited strong positive correlations with DC FTIR (r = 0.618) and Max Polymerisation Rate (r = 0.468). Volumetric Shrinkage had strong positive correlations with DC FTIR (r = 0.686). Additionally, it showed a strong negative correlation with Light Transmittance (r = − 0.550). Max Polymerisation Rate demonstrated a strong negative correlation with Time of Max Polymerisation Rate (r = − 0.684) and a strong positive correlation with Light Transmittance (r = 0.606). Total Porosity showed medium positive correlations with Filler Weight Percentage (r = 0.559).

5. Discussion

The aim of this study was to assess the adequacy of new state-of-the-art technology to evaluate a range of polymerisation-related properties of ten flowable and sculptable counterparts of commercial RBC materials. The results ascertain the applicability of O-PTIR for DC and micro-CT for PS measurements of depth-related changes in commercial RBCs. The results confirmed the high correlation of DC measured by FTIR and O-PTIR measurements at all depths, especially at 0 and 2 mm, thus confirming the applicability of O-PTIR for assessing DC changes with increasing distance from the light source. It was also found that higher filler content reduced DC and PS, while DC and PS were positively correlated. Furthermore, higher filler volume had a negative effect on R_{max} and a positive effect on total and closed porosity formation, but only a moderate impact on light transmittance.

This high **spatial** resolution is one of the distinguishing features of O-PTIR and makes it extremely effective for detailed surface analysis and mapping of chemical properties on a microscale [23]. This resolution is much finer than ATR-FTIR techniques, which generally have a spatial resolution in the range of several micrometres, determined primarily by the contact area between the ATR crystal and the sample and the dimensions of the evanescent wave, which penetrates only a few micrometres into the sample [21]. This makes ATR-FTIR less suitable for high-resolution mapping of heterogeneous materials, but very effective for bulk and sub-surface analysis. This was evident in the present study by the higher standard deviation of the DC measurements across depth by O-PTIR compared to the $DC_{5\ min}$ with ATR-FTIR. However, in terms of **spectral** resolution ATR-FTIR can achieve high spectral resolution, similar to other FTIR techniques, depending on the specific instrument settings and configurations [26].

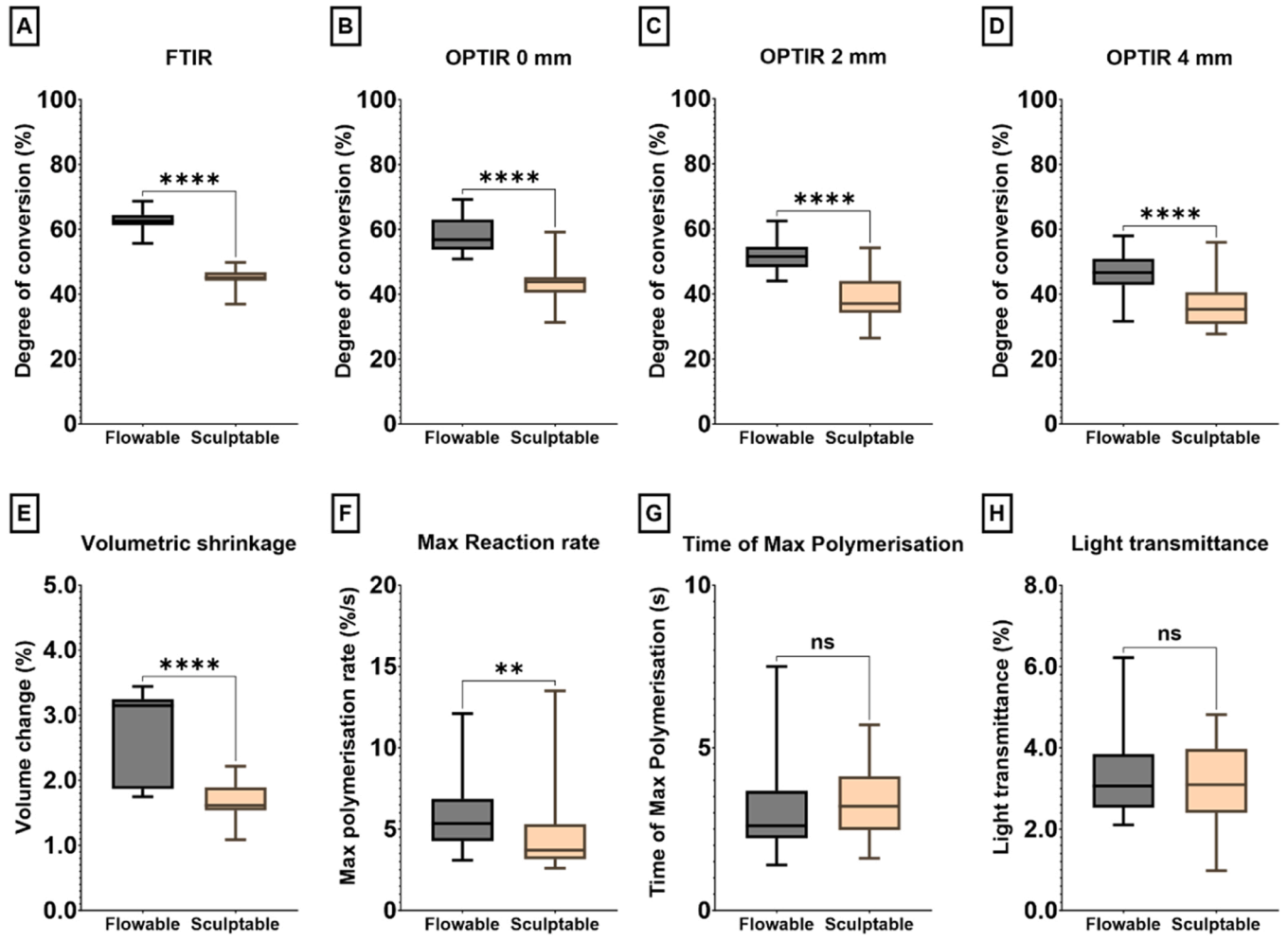

Fig. 9. Comparison of selected parameters between tested flowable and sculptable composites. *$p < 0.05$, ** $p < 0.01$, *** $p < 0.001$, **** $p < 0.0001$.

ATR-FTIR, on the other hand, enabled tracking time-dependent DC changes, including the polymerisation rate and the time to reach its maximum rate, under the current experimental conditions. In the present study, the unpolymerised material was used in direct contact with the diamond ATR crystal at 2 mm depth, light cured and the spectral changes over time were measured. The measurement of depth-dependent changes would also be possible with ATR-FTIR, but with repeated measurements and different samples for each depth (0, 2 and 4 mm). Although theoretically, the same sample could be used for repeated measurements, this is not easy to achieve in practice as close contact with the sample cannot always be re-established. The close contact between the ATR crystal and the sample can also be lost during the measurement due to contraction of the sample. In contrast, non-contact O-PTIR offers multiple measurements at different locations on the same sample at different times, allowing DC changes to be measured over a longer period of time. The spectra obtained with O-PTIR are similar to those of ATR-FTIR, so the same internal aromatic isosbestic point ($\sim 1608\ cm^{-1}$) can be used to calculate DC as with other FTIR and Raman spectroscopies. In our study, O-PTIR was also less sensitive to the change in optical path length due to PS than ATR-FTIR. The thickness of the sample is irrelevant for this technique as only surface effects are registered.

When discussing O-PTIR for DC determination in dental composites, an important point to address is the possible thermal effect of the infrared pulse at the sample surface on the post-cure DC changes. A large body of data confirms that the post-cure increase DC is amplified at higher temperatures [3,11,27], which is due to the increased mobility of unreacted monomers under the conditions of temperature-induced decrease in composite viscosity [3]. However, we found no increase in DC when comparing $DC_{5\ min}$, measured at 2 mm depth with ATR-FTIR, and $DC_{2\ mm}$, measured with O-PTIR. Instead, $DC_{2\ mm}$ values were generally lower than $DC_{5\ min}$. It must be emphasised that the same experimental conditions were ensured for both techniques, including the use of composite materials from the same batch and an identical curing device.

A high filler content in dental RBCs is desirable due to their reinforcing effect and the resulting higher strength, especially compressive strength, modulus of elasticity and hardness [14,18,27]. These properties are required for a restorative material that is intended to replace the dental structure in areas of high occlusal stress and other unfavourable conditions in the oral cavity although fracture toughness is the material property which predicts the best the clinical success of a restoration [28]. On the other hand, strong negative correlations between filler weight/volume fraction and DC were found in the present study (both FTIR and O-PTIR at all depths). These results are not surprising and are consistent with previous studies [29,30]. A higher filler content creates a spatial separation of the monomers by the filler particles and increased light scattering, which hinders the possibility of bringing the reactive groups of the monomers into close contact so that they can copolymerise. Reactive groups of the monomers can, however, react the corresponding reactive groups of the silane generated siloxane network on the surface of the filler particles. The higher viscosity in sculptable composites apparently impedes the monomer mobility in the pre-gel phase more than in flowable composites, as can be seen from the

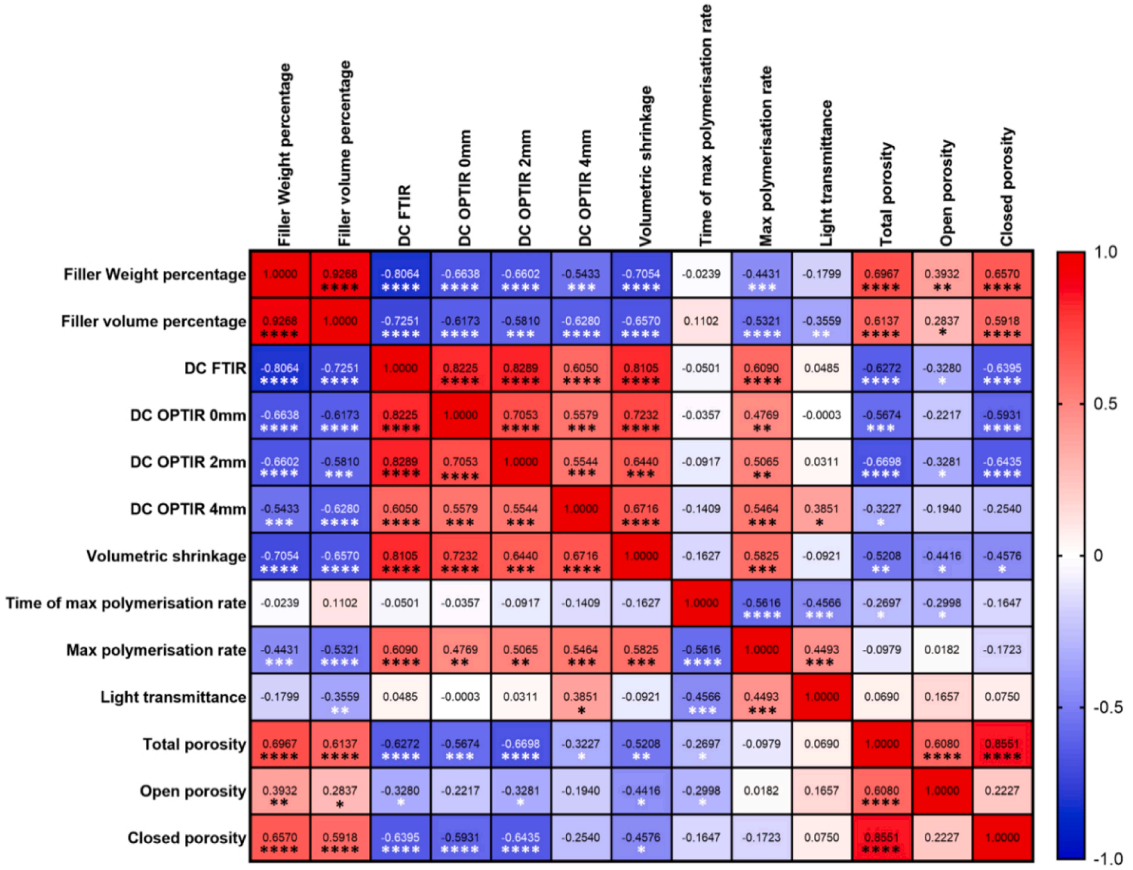

Fig. 10. Spearman Rank correlation shows the connection between the investigated parameters for all tested commercial composites. Small correlation if $0.1 < |r| < 0.3$; medium correlation if $0.3 < |r| < 0.5$; and strong correlation if $0.5 < |r| < 1$ [25], significance levels $^{*}p < 0.05$, $^{**}p < 0.01$,$^{***}p < 0.001$, $^{****}p < 0.0001$.

significantly lower R_{max} values for sculptable RBCs. In the present study, one flowable composite contained a higher filler content than the other flowable materials (G-aenial Universal Flow 69 wt%/59 vol%) and is indicated even for high-bearing areas (Class I–V). Regardless of the amount of filler, this material retained the DC, PS and R_{max} properties of the flowable group. This suggests that composites of this kind should be used in thin layers to avoid shrinking stress and deteriorating bonding to cavity walls. On the other hand, the shrinking stress depends on the composite's modulus of elasticity. In this respect, flowable resin composites with a lower modulus of elasticity may generate less shrinking stress to the bonding interface than sculptable composites with a higher modulus of elasticity.

The correlations between filler load and DC were generally stronger for FTIR measurements than for O-PTIR measurements, possibly due to the slightly larger standard deviations for O-PTIR. With the spot size of ~ 500 nm in O-PTIR and the higher sensitivity compared to FTIR microscopy [21], the IR laser used in O-PTIR could target not only the resin but also filler particles or the resin surrounding the fillers. Sirovica et al. found a heterogeneity of the polymer network with poorly polymerised areas around the filler particles in RBCs with non-silanised filler particles [31]. This feature may have led to some variability in the results obtained. However, due to the same feature, O-PTIR can be used for DC mapping the entire sample surface. This study focussed on the depth-related changes in DC in specific areas, from the subsurface (0 mm) up to 2- and 4-mm. DC mapping is time-consuming and cannot provide information on time-dependent changes during and after light polymerisation. On the other hand, ATR-FTIR is an established method that is fast enough to record the polymerisation kinetic behaviour [13, 32]. Therefore, these two methods can complement each other to gain insight into spatio-temporal events during and after polymerisation of the RBCs. In general, DC values of the composites studied here were of the same range which have been reported previously [33].

The present study observed a depth-dependent reduction of the DC, a phenomenon more pronounced in sculptable composites. All tested flowable/sculptable material combinations of the same brand showed a significantly lower DC at a depth of 4 mm, except the bulk-fill composites Filtek One Restorative Bulk Fill and Filtek Restorative Bulk Fill Flowable. This result is to be expected as the other materials tested are conventional RBCs, which are only designed for applications up to 2 mm. Bulk-fill composites, on the other hand, clearly exhibited the highest light transmittance in this study. This property was probably responsible for their high depth of cure, as evidenced by the statistically homogeneous values for $DC_{0\,mm}$, $DC_{2\,mm}$, and $DC_{4\,mm}$, which O-PTIR measured. The high light transmittance of Filtek Restorative Bulk Fill Flowable was probably also the reason for its fast polymerisation (high R_{max} and short t_{Rmax}). Since fast polymerisation does not allow for flow and adaptation of the material in the pre-gel phase, elastic modulus and possible negative effects on the development of shrinkage stress should be investigated in the future. Therefore, the clinical application of these bulk fill materials in 4 mm layers is scientifically valid with regard to their polymerisation-related properties tested here.

In this study, low filler content correlated with high volumetric PS, suggesting that flowable composites tend to have higher PS than their sculptable counterparts. However, there was no clear trend towards higher PS for materials with lower filler content in each group (sculptable or flowable). Rather, the relationship between DC and PS was clearly recognisable: materials with the highest DC also had the highest PS. The variability in total PS among the flowable materials was low (1.46–1.97 %), with almost no differences between them, with the exception of Brilliant EverGlow Flow. In contrast, the PS value of the sculptable materials varied between 2.23 % and 3.81 %.

The measurement of volumetric PS using micro-CT is not new and

has been used for over a decade [34,35]. The superposition of scans before/after curing with radiopaque fillers or tracing internal porosities is a valuable method for understanding shrinkage directions in bonded or unbonded cavities. It is generally agreed that the shrinkage vectors in bonded cavities are directed towards the bonded interface. The free surface becomes concave and has raised edges due to the material flow in the pre-gel phase [36,37]. However, in unbonded cavities, such as the one in the present study, shrinkage is directed towards the light source, with significant movement occurring at the bottom of the cavity. However, the shrinkage vectors depend on the DC when the sample size exceeds the RBC's cure depth [36]. Our results are in good agreement with previous studies [30,38,39], with greater PS observed in the flowable composites than in the sculptable composites. A qualitative leakage study showed dye penetration from top to bottom [40], suggesting increased shrinkage at the base, especially for flowable RBCs, which are known for higher shrinkage values [41]. The added benefit of this study is that it is a new post-processing method for analysing before/after micro-CT scans that do not require special preparation of the materials or detection of air entrapment. Nevertheless, it can provide quantitative measurements of PS at different depths of cure.

Two excellent proposals for new methods to assess PS have recently been published [33,42]. Similar to the present study, commercial RBCs were tested in both studies. In contrast to the present study, Szczesio-Wlodarczyk et al. did not find a significant correlation between the weight or volume of the filler and PS [33]. A possible explanation for this could be the different resin matrix systems and innovative filler types used in these studies, which apparently had a more decisive influence on PS properties than the amount of filler. In the present study, the combination of flowable and sculptable same brand RBCs was used, assuming that a similar resin matrix and filler type were used for materials of the same brand. The correlation tables for separate flowable and sculptable materials used in this study can be found in the appendix. They show only weak, non-significant correlations (except filler wt% and $DC_{5\ min}$ for sculptable materials). In addition to the different resin matrix systems, the relatively small variations in filler content could also be responsible for these results.

This study enhances our understanding of the nuanced performance characteristics of dental composites. Using O-PTIR and micro-CT provides novel insights into material properties that traditional methods do not easily capture.

The study's findings testify to the importance of a multi-technique analytical approach in discerning the subtleties of dental composite performance. The observed variability in physical and chemical properties across flowable and bulk composites underscores the nuanced decision-making process in material selection for dental restorations. These insights could guide the optimisation of composite formulations, aiming to strike an optimal balance between ease of application, curing efficiency, and the mechanical integrity of the resultant restorations.

6. Conclusion

This study used advanced analytical techniques such as micro-CT and optical photothermal infrared spectroscopy (O-PTIR) to comprehensively compare flowable and sculptable dental resin-based composites of the same brand. The key findings reveal that composites with lower filler content (flowables) generally exhibit a higher degree of conversion (DC) and faster polymerisation rates than sculptable composites. However, this advantage is compromised by the increased volumetric polymerisation shrinkage (PS), which has significant implications for the clinical use of these materials. The findings underscore the importance of a multi-technique approach to fully understanding dental composites' behaviour. Integrating O-PTIR and micro-CT has provided novel insights that traditional methods might overlook, particularly in mapping DC variations and visualising shrinkage patterns in three dimensions.

Acknowledgements

This work was supported by the Croatian Science Foundation [grant number IP-2019–04-6183, ″Biomimetic intelligent composite systems″].

Appendix A. Supporting information

Supplementary data associated with this article can be found in the online version at doi:10.1016/j.dental.2024.09.002.

References

[1] Opdam NJ, van de Sande FH, Bronkhorst E, Cenci MS, Bottenberg P, Pallesen U, et al. Longevity of posterior composite restorations: a systematic review and meta-analysis. J Dent Res 2014;93:943–9.
[2] Watts DC. Reaction kinetics and mechanics in photo-polymerised networks. Dent Mater 2005;21:27–35.
[3] Stansbury JW. Dimethacrylate network formation and polymer property evolution as determined by the selection of monomers and curing conditions. Dent Mater 2012;28:13–22.
[4] Marovic D, Bota M, Tarle F, Par M, Haugen HJ, Zheng K, et al. The influence of copper-doped mesoporous bioactive nanospheres on the temperature rise during polymerization, polymer cross-linking density, monomer release and embryotoxicity of dental composites. Dent Mater 2024.
[5] Haugen HJ, Marovic D, Par M, Thieu MKL, Reseland JE, Johnsen GF. Bulk fill composites have similar performance to conventional dental composites. Int J Mol Sci 2020;21.
[6] Kopperud HM, Johnsen GF, Lamolle S, Kleven IS, Wellendorf H, Haugen HJ. Effect of short LED lamp exposure on wear resistance, residual monomer and degree of conversion for Filtek Z250 and Tetric EvoCeram composites. Dent Mater 2013;29:824–34.
[7] Arikawa H, Kanie T, Fujii K, Takahashi H, Ban S. Effect of filler properties in composite resins on light transmittance characteristics and color. Dent Mater J 2007;26:38–44.
[8] Dennison JB, Sarrett DC. Prediction and diagnosis of clinical outcomes affecting restoration margins. J Oral Rehabil 2012;39:301–18.
[9] Kidd EA, Joyston-Bechal S, Beighton D. Marginal ditching and staining as a predictor of secondary caries around amalgam restorations: a clinical and microbiological study. J Dent Res 1995;74:1206–11.
[10] Khvostenko D, Salehi S, Naleway SE, Hilton TJ, Ferracane JL, Mitchell JC, et al. Cyclic mechanical loading promotes bacterial penetration along composite restoration marginal gaps. Dent Mater 2015;31:702–10.
[11] Par M, Gamulin O, Marovic D, Klaric E, Tarle Z. Effect of temperature on post-cure polymerization of bulk-fill composites. J Dent 2014;42:1255–60.
[12] Par M, Gamulin O, Marovic D, Klaric E, Tarle Z. Raman spectroscopic assessment of degree of conversion of bulk-fill resin composites–changes at 24 h post cure. Oper Dent 2015;40:E92–101.
[13] Marovic D, Par M, Tauböck TT, Haugen HJ, Negovetic Mandic V, Wüthrich D, et al. Impact of copper-doped mesoporous bioactive glass nanospheres on the polymerisation kinetics and shrinkage stress of dental resin composites. Int J Mol Sci 2022;23:8195.
[14] Son SA, Park JK, Seo DG, Ko CC, Kwon YH. How light attenuation and filler content affect the microhardness and polymerization shrinkage and translucency of bulk-fill composites? Clin Oral Invest 2017;21:559–65.
[15] Par M, Repusic I, Skenderovic H, Sever EK, Marovic D, Tarle Z. Real-time light transmittance monitoring for determining polymerization completeness of conventional and bulk fill dental composites. Oper Dent 2018;43:E19–31.
[16] Oberholzer TG, Pameijer CH, Grobler SR, Rossouw RJ. Volumetric polymerisation shrinkage of different dental restorative materials. Sadj 2004;59:8–12.
[17] Choi KK, Ferracane JL, Hilton TJ, Charlton D. Properties of packable dental composites. J Esthet Dent 2000;12:216–26.
[18] Mirică IC, Furtos G, Bâldea B, Lucaciu O, Ilea A, Moldovan M, et al. Influence of filler loading on the mechanical properties of flowable resin composites. Materials 2020;13.
[19] Kitasako Y, Sadr A, Burrow MF, Tagami J. Thirty-six month clinical evaluation of a highly filled flowable composite for direct posterior restorations. Aust Dent J 2016;61:366–73.
[20] Haugen HJ, Ma Q, Linskens S, Par M, Mandic VN, Taubock TT, et al. 3D Micro-CT and O-PTIR Spectroscopy Bring New Understanding of the Influence of Filler Content in Dental Resin Composites. Dent Mater 2024. https://doi.org/10.1016/j.dental.2024.09.001.
[21] Chua L, Banas A, Banas K. Comparison of ATR-FTIR and O-PTIR imaging techniques for the characterisation of zinc-type degradation products in a paint cross-section. Molecules 2022;27.
[22] Sandt C, Borondics F. Super-resolution infrared microspectroscopy reveals heterogeneous distribution of photosensitive lipids in human hair medulla. Talanta 2023;254:124152.
[23] Kansiz M, Prater C, Dillon E, Lo M, Anderson J, Marcott C, et al. Optical photothermal infrared microspectroscopy with simultaneous Raman – a new non-contact failure analysis technique for identification of < 10 μm organic contamination in the hard drive and other electronics industries. Micros Today 2020;28:26–36.

[24] Munir A, Marovic D, Nogueira LP, Simm R, Naemi AO, Landro SM, et al. Using copper-doped mesoporous bioactive glass nanospheres to impart anti-bacterial properties to dental composites. Pharmaceutics 2022;14.
[25] Cohen J. Set correlation and contingency-tables. Appl Psych Meas 1988;12:425–34.
[26] Kim D, Townsley S, Grassian VH. Vibrational spectroscopy as a probe of heterogeneities within geochemical thin films on macro, micro, and nanoscales. RSC Adv 2023;13:28873–84.
[27] Ilie N, Hickel R. Investigations on mechanical behaviour of dental composites. Clin Oral Invest 2009;13:427–38.
[28] Heintze SD, Ilie N, Hickel R, Reis A, Loguercio A, Rousson V. Laboratory mechanical parameters of composite resins and their relation to fractures and wear in clinical trials–a systematic review. Dent Mater 2017;33:e101–14.
[29] Czasch P, Ilie N. In vitro comparison of mechanical properties and degree of cure of a self-adhesive and four novel flowable composites. J Adhes Dent 2013;15:229–36.
[30] Nunes TG, Pereira SG, Kalachandra S. Effect of treated filler loading on the photopolymerization inhibition and shrinkage of a dimethacrylate matrix. J Mater Sci Mater Med 2008;19:1881–9.
[31] Sirovica S, Solheim JH, Skoda MWA, Hirschmugl CJ, Mattson EC, Aboualizadeh E, et al. Origin of micro-scale heterogeneity in polymerisation of photo-activated resin composites. Nat Commun 2020;11:1849.
[32] Par M, Tarle Z, Hickel R, Ilie N. Polymerization kinetics of experimental bioactive composites containing bioactive glass. J Dent 2018;76:83–8.
[33] Szczesio-Wlodarczyk A, Garoushi S, Vallittu P, Bociong K, Lassila L. Polymerization shrinkage of contemporary dental resin composites: comparison of three measurement methods with correlation analysis. J Mech Behav Biomed Mater 2024;152:106450.
[34] Ghavami-Lahiji M, Davalloo RT, Tajziehchi G, Shams P. Micro-computed tomography in preventive and restorative dental research: a review. Imaging Sci Dent 2021;51:341–50.
[35] Sun J. Lin-Gibson S. X-ray microcomputed tomography for measuring polymerization shrinkage of polymeric dental composites. Dent Mater 2008;24:228–34.
[36] Cho E, Sadr A, Inai N, Tagami J. Evaluation of resin composite polymerization by three dimensional micro-CT imaging and nanoindentation. Dent Mater 2011;27:1070–8.
[37] Kweon HJ, Ferracane J, Kang K, Dhont J, Lee IB. Spatio-temporal analysis of shrinkage vectors during photo-polymerization of composite. Dent Mater 2013;29:1236–43.
[38] Miyasaka T, Okamura H. Dimensional change measurements of conventional and flowable composite resins using a laser displacement sensor. Dent Mater J 2009;28:544–51.
[39] Goncalves F, Kawano Y, Braga RR. Contraction stress related to composite inorganic content. Dent Mater 2010;26:704–9.
[40] Par M, Prskalo K, Taubock TT, Skenderovic H, Attin T, Tarle Z. Polymerization kinetics of experimental resin composites functionalized with conventional (45S5) and a customized low-sodium fluoride-containing bioactive glass. Sci Rep 2021;11:21225.
[41] de Gee AF, Feilzer AJ, Davidson CL. True linear polymerization shrinkage of unfilled resins and composites determined with a linometer. Dent Mater 1993;9:11–4.
[42] Chen W-C, Lai T-W, Li C-L, Chen TY-F, Chang C-H, Chuang S-F. Assessments of polymerization shrinkage by optical coherence tomography-based digital image correlation analysis—Part II: effects of restorative composites. Dent Mater 2024.